NASA-TM-83984 19830010813

A Reproduced Copy

OF

NASA TM- 83984

Reproduced for NASA

by the

NASA Scientific and Technical Information Facility

FFNo 672 Aug 65

NASA

Technical Memorandum 83984

The Airborne Laser Ranging System, Its Capabilities and Applications

W. D. Kahn, J. J. Degnan and T. S. Englar, Jr.

SEPTEMBER 1982

THE AIRBORNE LASER RANGING SYSTEM,

ITS CAPABILITIES AND APPLICATIONS

By

W. D. Kahn
J. J. Degnan
Goddard Space Flight Center
Greenbelt, MD 20771

T. S. Englar, Jr.
Business and Technological Systems, Inc.
Seabrook, MD 20801

THE AIRBORNE LASER RANGING SYSTEM,

ITS CAPABILITIES AND APPLICATIONS

By

W. D. Kahn

J. J. Degnan

Goddard Space Flight Center
Greenbelt, MD 20771

T. S. Englar, Jr.

Business and Technological Systems, Inc.

Seabrook, MD 20801

ABSTRACT

The Airborne Laser Ranging System is a proposed multibeam short pulse laser ranging system on board an aircraft. It simultaneously measures the distances between the aircraft and six laser retroreflectors (targets) deployed on the Earth's surface (Figure 1). The system can interrogate over 100 targets distributed over an area of 2.5×10^4 sq. kilometers in a matter of hours. Potentially, a total of 1.3 million individual range measurements can be made in a six hour flight. The precision of these range measurements is approximately ± 1 cm (1). These measurements are then used in a procedure which is basically an extension of trilateration techniques to derive the intersite vector between the laser ground targets. By repeating the estimation of the intersite vector, strain and strain rate errors can be estimated. These quantities are essential for crustal dynamic studies which include determination and monitoring of regional strain in the vicinity of active fault zones, land subsidence, and edifice building preceding volcanic eruptions.
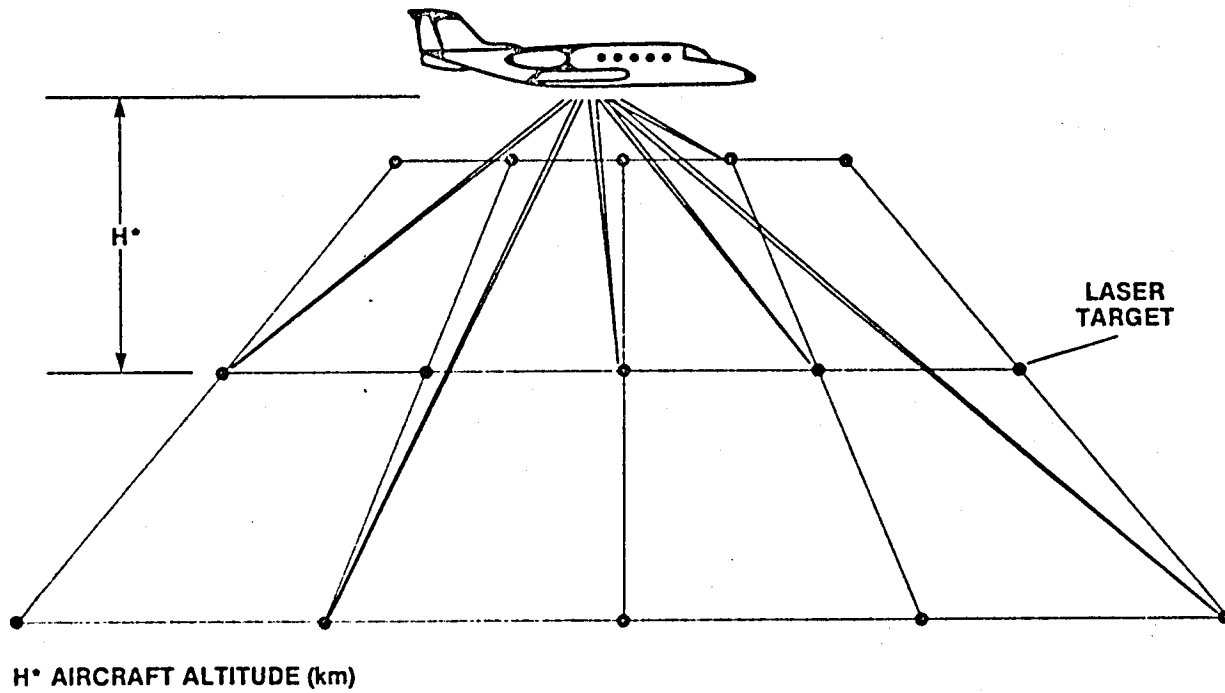
H° AIRCRAFT ALTITUDE (km)

Figure 1. Airborne Laser Ranging System Concept

THE AIRBORNE LASER RANGING SYSTEM,
ITS CAPABILITIES AND APPLICATIONS

1.0 INTRODUCTION

Recent experience with laser and Very Long Baseline Interferometer (VLBI) measurements in Southern California reveal that large scale crustal motions can occur in time scales of a few weeks and months. To adequately monitor such motion, techniques are required to map the position of grid points over a region in a few days and at repeat frequencies of a few weeks. In addition, maps of crustal deformation rates encompassing 20 to 40 locations are required within several days of the observations. The monitoring of relative motions in the Earth's upper crust in tens to sub-centimeter rate per year can be accomplished by a pulsed laser ranging system carried on-board an aircraft, making rapid range measurements to passive reflectors distributed on the ground. By developing and interpreting this system's ability to detect motions of the Earth's upper crust, a model of the strain accumulation compatible with observations of crustal motion and tectonics of a region within the experimental data collection area can be derived. Furthermore, an Air-borne Laser Ranging System (ALRS) can survey an area in a very short period of time (hrs.) and resurvey the areas as required.

The basic philosophy of the Airborne Laser Ranging System is to invert the usual laser ranging configuration by placing the ranging and pointing hardware in an aircraft such as NASA's NP3A Lockheed Orion Research Aircraft, and replacing the expensive laser ground stations by low cost (< $1000) passive retroreflectors. The system is necessarily multibeam since the location of the aircraft is not known with cm precision at each point where a set of range measurements are made. Thus, a minimum of four simultaneous range measurements are required, i.e., three to resolve the new coordinates of the aircraft and one to acquire information on the relative locations of the ground targets. The ALRS system will be capable of ranging simultaneously to six retroreflectors. At a laser repetition rate of 10pps, a potential 1.3 million individual range

measurements can be made and an area as large as 60,000 sq. km can be surveyed during one six hour flight. The latter coverage applies to a high altitude research aircraft such as an RB-57 or U2 which can operate at altitudes above 18 km and is reduced for aircraft having lower operational altitudes.

Computer simulations have shown that in the presence of measurement noise and bias coupled with tropospheric refraction effects, an aircraft operating at a more modest maximum altitude of 6 km, can determine intersite distances to a precision of 0.4 cm at 5 km and 1.4 cm at 30 km baseline distances. The error growth rate per unit baseline varies inversely with aircraft altitude. Furthermore, the data reduction technique simultaneously resolves the aircraft position to the cm level at each point in the flight path where a laser pulse is transmitted. The ALRS system is expected to be a powerful new research tool for monitoring regional crustal motion, land management applications, and general surveying because it will provide a "snapshot" of the target positions over an extended area with high spatial resolution.

2.0 SYSTEM DESCRIPTION

2.1 Laser Ranging Subsystem

Figure 2 is a block diagram of the ALRS. The system computer enables the firing of a sub-nanosecond laser transmitter at a nominal rate of 10 pps. The transmitter is a modelocked, PTM Q-switched Nd:YAG laser oscillator followed by a double-pass Nd:YAG laser amplifier and a KD*P frequency doubler. On each firing, the transmitter generates a single 150 psec (FWHM) pulse containing several millijoules of energy at the 0.532 micrometer green wavelength. A beamsplitter reflects a very small fraction ($< 1\%$) of the outgoing energy into a series of six beamsplitters which divide and direct the low-level energy into each of six receiver channels. The remaining energy is divided into approximately six equal parts by a second set of beamsplitters which directs the energy to six independently controlled pointing systems. The six outgoing pulses pass through the atmosphere to illuminate six ground target retroreflectors. The reflected energy

2

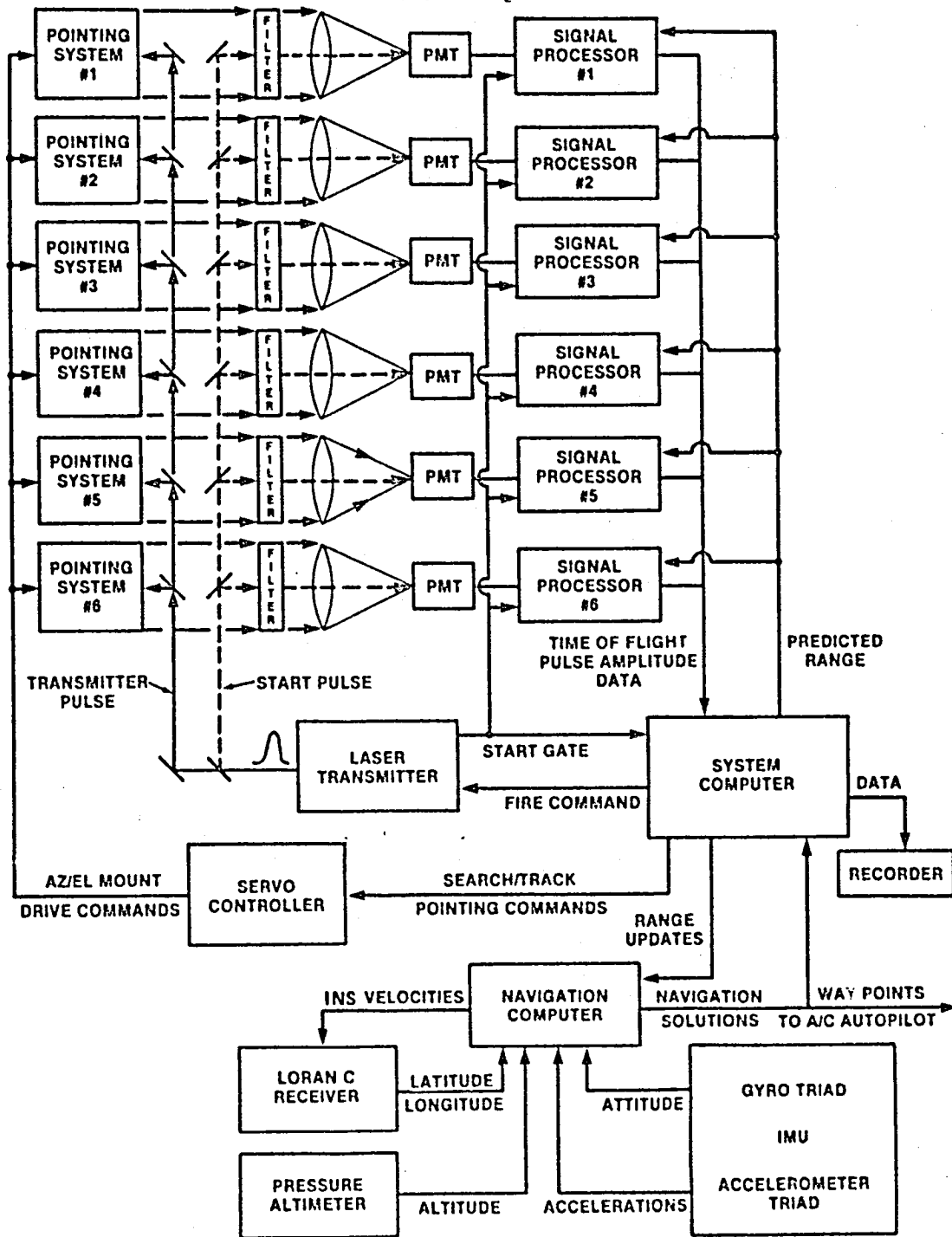Figure 2. Block Diagram of the Airborne Laser Ranging System

3

from each target travels back through the atmosphere to the ALRS and is imaged onto the corresponding high speed photomultiplier tube (PMT). Thus, a pair of start and stop pulses, indicating the times at which a given pulse leaves and returns to the instrument, are recorded by each of the six receiver channels. The use of common start/stop receiver components eliminates a potential source of time–dependent range bias which might be introduced by changes in the thermal environment, voltage condition, or other nonstationary processes during flight.

The output of each PMT is split inside the signal processor. One port is input to a low time walk constant fraction discriminator. The discriminator provides a NIM logic pulse to both start, and later stop, one channel of a multichannel time interval unit. The latter device measures the time–of–flight for each of the six laser pulses. The six channels in the TIU share a common clock input. The range to each target is calculated from time–of–flight with suitable corrections being made for instrument biases, pulse amplitude effects, and atmospheric refraction delays. A charge digitizer at the second port of the PMT output records the energies of the outgoing (START) and incoming (STOP) pulses thereby enabling the system computer to correct for timing biases due to pulse amplitude (dynamic range) effects. The measurement data is transferred to the system computer for storage and use by the navigational subsystem as described in Section 2.3. Nominal atmospheric refraction corrections are made inflight for use by the navigation computer. More exact corrections are made during the post–flight data reduction phase.

Instrument related single–shot range uncertainties are about 5 mm RMS (one sigma) with an average received signal level of 200 photoelectrons. This is the signal level calculated for a worst-case link which assumes 1 mJ of laser energy per channel, a 0.5° beam divergence, and a minimum aircraft elevation angle of 20° as viewed by a ground target with a modest cross–section of 10^6m^2. The aircraft is assumed to be at its maximum altitude of 6 km.

The laser transmitter, beam splitting optics, receiver optics, and photomultiplier tubes are mounted on an optical baseplate which is isolated vibrationally from the aircraft fuselage. Six azimuth-elevation pointing mounts with 5 cm receive apertures are rigidly attached to the bottom of the optical bed. Each pointing system consists of a four mirror coelostat mounted on an azimuthally rotating stage as in Figure 3. The laser beam enters the pointing system through a hole in the optical baseplate and the rotation stage. The final mirror rotates about an axis parallel to the optical bench to point to a given elevation angle. This particular configuration was chosen because it can be placed very close to the aircraft window to provide near hemispherical
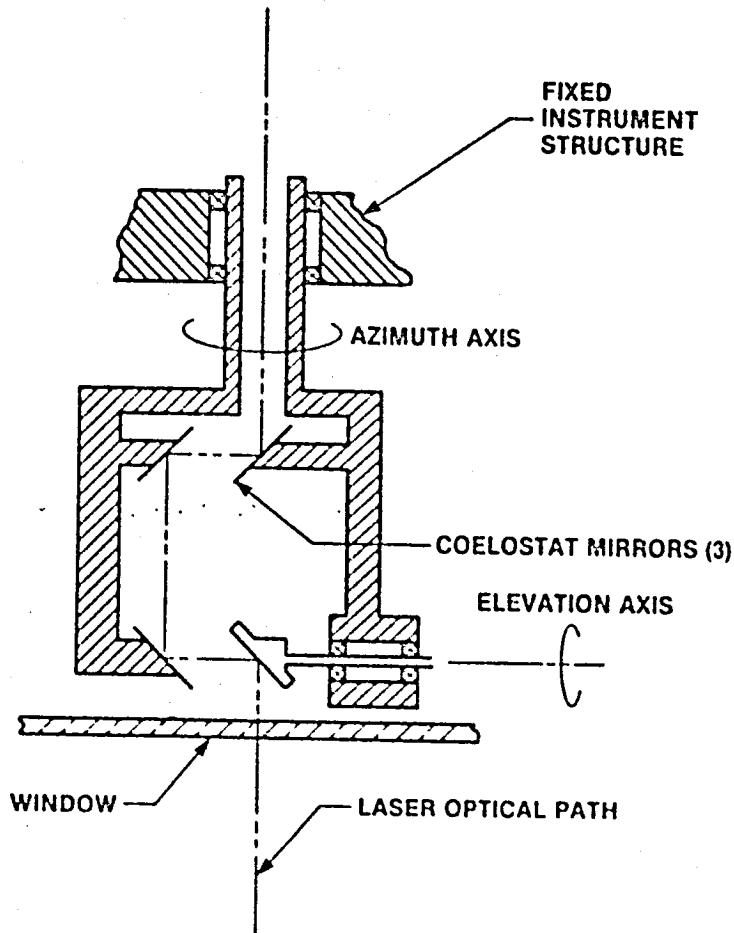
FIXED
INSTRUMENT
STRUCTURE

AZIMUTH AXIS

COELOSTAT MIRRORS (3)

ELEVATION AXIS

WINDOW

LASER OPTICAL PATH

Figure 3. Optical Pointing System Concept

5

viewing capability. A second advantage is that all light beams reflect at a 45° incidence angle independent of the AZ/EL pointing angles. This allows the use of high efficiency dielectric coatings on the mirrors for maximum receiver sensitivity and potential upgrade of the system to two colors for making direct measurements of the atmospheric refraction correction. (1)

Each pointing mount is equipped with two servo systems (azimuth and elevation). In the present concept, these systems are digital controllers that drive precision stepping motors and contain optical encoders to measure angular position. The commands sent to the controller are in the form of angular position, velocity, and acceleration referred to the optical bench. The controller performs the usual loop closure tasks to control the individual servos as directed and to relay information back to the command interface. Command angles and predicted range gates are generated by the system computer using aircraft navigation solutions provided by the navigation and attitude determination subsystem.

With laser beam divergences on the order of several milliradians, absolute pointing accuracies at the mrad level are adequate. This performance is a factor 10 to 20 times less stringent than typically required for ground-based satellite laser ranging systems.

2.2 Target Deployment

A number of geodetic monuments will be erected in the region of interest. The "grapefruit-sized" targets, studded with about six optical cube corners, can be mounted directly on the monuments prior to the survey flight. These can be either permanent installations or the targets can be removed and reused at other locations. In order to tie the target grid accurately to a reference coordinate system targets would be placed at three or more fiducial points. To simplify the target acquisition sequence, it is desirable that the position of each target be known apriori to approximately 50 meters but this is not a hard requirement. The apriori knowledge of target position does not impact the aposteriori grid resolution achieved by the ALRS. In

general, apriori location can be read from a surveyors map or obtained using radio navigation receivers such as Loran C, the TRANSIT Satellite System, or the future Global Positioning System (GPS).

2.3 Target Acquisition and Tracking

The a priori target positions discussed in the previous section will be stored in the ALRS system computer memory as latitude, longitude, and altitude above sea level. Successful acquisition and tracking of the targets during flight requires an adequate knowledge of the aircraft position, velocity, and attitude. The positional error in a modern inertial navigation system (INS) typically grows at a rate of 0.4 to 4.0 km/hour. In such a system, vehicle accelerations and attitude are measured by an inertial measurement unit (IMU) consisting of three orthogonal accelerometers and a gyro triad. The navigational computer (NC) performs coordinate transformations and integrates the equations of motion to provide estimates of velocity and position relative to a set of initial conditions. The errors in these estimates have many contributing sources including sensor calibration limitations and inaccuracies, computational errors, and sensor-error-propagation effects.

The performance of an INS can be improved significantly by incorporating additional independent sensors which periodically check and update the navigation solutions. Radio navigation aids (such as OMEGA, LORAN C, and the future GPS system) are particularly well suited to the role of auxiliary sensor because of their global or near global coverage. In the ALRS, latitude and longitude information from a LORAN C receiver is utilized to update and stabilize the corresponding INS solutions via a Kalman filter algorithm in the NC (2). Similarly, barometric altimeter measurements of altitude are processed in the NC to stabilize the equations for vertical velocity and altitude. The Kalman filter also updates attitude information and provides best estimates of sensor errors such as misalignments, accelerometer biases and scale factors, gyro drift rates, etc. The INS velocity solution assists the LORAN C receiver in the acquisition of Doppler-shifted

signals from the LORAN ground network. In the event of certain types of failure, the proposed navigational system can be restarted and calibrated in flight.

Flight tests of a LORAN-aided INS (3) performed for the U.S. Air Force have demonstrated a 60 meter absolute position accuracy (one sigma) and a 15 meter RMS random noise error (one sigma) and angular accuracies of a few tenths of a milliradian. LORAN C was chosen for the ALRS because it is significantly more accurate than OMEGA (±925 meters) and, unlike GPS, is already available in most regions of the world. The Global Positioning System will eventually provide more accurate dynamic fixes in all three coordinates (5 meters) and global coverage, but the system is unlikely to become fully operational before 1988.

The navigational data is combined with the stored a priori target positions to compute the estimated range gates and the pointing mount command angles. As the targets come within range, the laser is activated and the presence or absence of range returns is noted. If no returns are detected, a search pattern is executed until range data is acquired. Selected range data is then passed to the navigation Kalman filter to update the estimate of aircraft position. The ALRS then shifts from the acquisition to the tracking mode.

In the tracking mode, triangulation on the highly accurate laser returns results in an aircraft position estimate which is virtually error free (better than a meter standard deviation) so that, except for aircraft attitude estimation errors contributed by the gyros, the computed command angles and range gates are essentially correct. The instrument remains in the tracking mode as long as sufficient range data is available to maintain an accurate estimate of aircraft position. In making the transition to a new set of six targets, the system triangulates on laser returns which are common to the new and the previous set. In this way, the aircraft position is known with better than meter accuracy during the transition. The design of the system computer and a description of the inflight operational software is given elsewhere. (4)

8

3.0 MATHEMATICAL MODELS AND ALGORITHMS

The mathematical model associated with the data generated by the ALRS system will be given in this section. This model will lead to the definition of an estimation algorithm for the coordinates of the retroreflector positions.

3.1 Range Data Model

Ideally, the ranging system measures the distance (range) between the airborne laser and several retroreflectors deployed on the Earth's surface.

Let $Z_{(3 \times 1)}(t)$ and $\dot{Z}_{(3 \times 1)}(t)$ be the 3-dimensional vectors describing the position and velocity of the aircraft at time t,

$$Z_{(3 \times 1)}(t) = \begin{bmatrix} z_1(t) \\ z_2(t) \\ z_3(t) \end{bmatrix}_{(3 \times 1)} \quad \text{and} \quad \dot{Z}_{(3 \times 1)}(t) = \begin{bmatrix} \dot{z}_1(t) \\ \dot{z}_2(t) \\ \dot{z}_3(t) \end{bmatrix}_{(3 \times 1)} \tag{1.0}$$

The vector components are expressed in some convenient, coordinate system.

Also let,

$$U^{(k)}_{(3 \times 1)} = \begin{bmatrix} u_1^{(k)} \\ u_2^{(k)} \\ u_3^{(k)} \end{bmatrix}_{(3 \times 1)} \tag{1.1}$$

be the 3-dimensional vector describing the position of the kth retroreflector in the same coordinate system.

The distance between the kth retroreflector and the airborne laser at time t is:

$$d(t, k) = [Z^T(t) Z(t) + U^{(k) T} U^{(k)} - 2Z^T(t) U^{(k)}]^{1/2} \tag{1.2}$$

Equation (1.2) does not completely represent the model for the ALRS measurements since the accuracy goals specified for the system require that this model be considerably refined.

The principal difference between d(t, k) and the ALRS measurement is the refraction increment r(t, k); however the model used for ALRS also includes a measurement bias, b_i, on the ith

9

beam, and a random error, v, which is uncorrelated in time or between beams. Thus the ALRS range measurement model is given by

$$\rho(t, k, i) = d(t, k) + r(t, k) + b_i + v(t, k, i) \tag{1.3}$$

where

$t \equiv$ time that measurement is made

$k \equiv$ retroreflector illuminated at time t

$i \equiv$ beam used.

The purpose of the ALRS measurement algorithm is to process the range data $(\rho_1, \rho_2, \ldots, \rho_n)$ and produce an estimate of the retroreflector positions $U_{(3N_r \times 1)}$. It is clear that this must be accompanied, at least implicitly, by estimates of the aircraft positions $Z(t_\ell)$ at the measurement times, t_ℓ. Furthermore, the refraction and the biases must be modelled, and their effects compensated.

The biases are modelled as stationary constants to be estimated. The refraction increment $r(t, k)$ is more difficult to analyze. However, the basic model for $r(t, k)$ is that previously used for analysis of satellite laser ranging (5) which was derived by Gardner in (6) and (7).

For ALRS purposes, the aircraft height has been included in the model, but since more recent studies by Gardner (8) have indicated that errors in $r(t, k)$ do not depend upon azimuth, the existing formulation shows refraction compensation errors to depend upon barometric pressure and the gradient of PTK (i.e., pressure X temperature X coefficient related to lapse time) (9, 10).

Variables which appear in the estimation process are collectively referred to as the estimation state, denoted by X, that is

$$X_{N \times 1} \equiv \begin{bmatrix} U^{(1)} \\ U^{(2)} \\ \vdots \\ U^{(N_r)} \\ Z(t) \\ \dot{Z}(t) \\ b_1 \\ \vdots \\ b_{N_B} \\ p_1 \\ \vdots \\ p_{N_r} \\ q_1 \\ \vdots \\ q_{N_r} \end{bmatrix}_{N \times 1} \tag{1.4}$$

where

$$N = 5N_r + N_B + 6$$

and

$p_k, q_k \equiv$ respectively, the pressure and gradient PTK at the kth retroreflector site

$N_B \equiv$ the number of independent laser beams

$N_R \equiv$ the number of retroreflector sites

The inclusion of $\dot{Z}(t)$ will be explained below.

3.2 The Estimation Process

An enormous quantity of data can be acquired during an ALRS aircraft flight. For a six hour flight, the system can operate at a repetition rate of 10 pps and receive return pulses on six (N_B) beams to register nearly 1.3 million range measurements. This aspect alone rules out any "Batch Processing" technique in which a large information matrix is inverted to estimate all parameters at once. A sequential estimation process (minimum variance/Kalman filter) has therefore been developed, in which each return, or the N_B returns from a single pulse, are used to modify the existing estimate of $X_{N \times 1}$. This approach has been assumed in the definition of $X_{(N \times 1)}$ above, where a time-varying aircraft position appears in the state, rather than a sequence of independent aircraft positions. In addition, it is assumed explicitly that during a single

11

ALRS flight, the other components of the state are constant; i.e., no crustal motion takes place, the beam biases remain the same, and the error in knowledge of atmospheric conditions at each retroreflector position remains unchanged.

At least four distinct concepts are involved in using a sequential algorithm:

(i) How to change a vector estimate, given a scalar measurement;

(ii) Modify (i) to include statistical error concepts;

(iii) How is the process to be initiated;

(iv) How are the time-varying aircraft positions handled.

These concepts are treated exhaustively in the literature, (11) among others; thus only a brief analysis will be discussed here.

The approach is fundamentally based on linearization. Because a prior estimate exists, an estimated or predicted range measurement $\hat{\rho}(t, k, i)$ can be computed, based on the estimated variables. The actual measurement is then represented in a truncated Taylor's series as:

$$\rho(t, k, i) = \hat{\rho}(t, k, i) + \frac{\partial \rho}{\partial X}\bigg|_{X=\hat{X}^-} (X - \hat{X}^-) + v \tag{1.5}$$

where a minus or plus superscript refers to instant, just before or just after the processing of data, respectively.

This now has the form,

$$y = h^T(X - \hat{X}^-) + v. \tag{1.6}$$

One important estimator is the Kalman filter, for which the optimum estimate is expressed by

$$(\hat{X}^+ - \hat{X}^-) = Ky \tag{1.7}$$

K being the optimum filter gain. The error, e, in the estimate is

12

$$\epsilon = (X - \hat{X}^-) - Ky = (X - \hat{X}^+) \tag{1.8}$$

and the covariance of this error is the expectation of $\epsilon\epsilon^T$:

$$P^+ = E(\epsilon\epsilon^T) \tag{1.9}$$

Since the variances of the error components are given by the diagonal elements of P, a minimum variance estimate is obtained by solving for those components of $(X - \hat{X})$ which minimize tr(P) that is:

$$\begin{aligned}
\text{tr}(P^+) &= \text{tr}[E(\epsilon\epsilon^T)] \\
&= \text{tr}\left\{ E(X - \hat{X}^-)(X - \hat{X}^-)^T - 2E(X - \hat{X}^-)y^T K^T + KE(yy^T)K^T \right\}
\end{aligned} \tag{1.10}$$

and

$$\frac{d(\text{tr } P)}{dK} = \left\{ -2E(X - \hat{X}^-)y^T + 2KE(yy^T) \right\} = 0. \tag{1.11}$$

Then

$$K = E(X - \hat{X}^-)y^T E(yy^T)^{-1} \tag{1.12}$$

where

$$E(X - \hat{X}^-)y^T = P^-h$$

$$E(yy^T) = [h^T P^- h + R]$$

$$E(vv^T) = R$$

Thus

$$K = P^-h[h^T P^- h + R]^{-1} \tag{1.13}$$

The matrix P^- is used in (1.13) to obtain the optimum filter gain, which in turn, is used to calculate the optimum estimate of the state from (1.7). A new value for this matrix is computed from

$$P^+ = (1 - Kh^T)P^- \tag{1.14}$$

where I is a unit matrix of proper dimensionality.

Then

$$\hat{X}^+ = \hat{X}^- + P^-h(h^T P^- h + R)^{-1} h^T P^-(\rho - \hat{\rho}) \tag{1.15}$$

The measurement, ρ, is not exact. There are inaccuracies involved in the pulse timing, modelling errors, etc. All of these error sources are lumped into the uncorrelated noise term (1.5) $v(t, k, i)$. On the basis that the primary source of this error is truncation noise in the clock and that b_i takes up the constant components, the statistical model for v introduced in (1.5) was selected with

$$E\left\{v(t, k, i)\right\} = 0$$

$$E\left\{v(t_m, k, i)\, v(t_n, l, j)\right\} = R\, \delta_n^m\, \delta_l^k\, \delta_j^i \tag{1.16}$$

where

$$\delta_n^m = \begin{cases} 0 & m \neq n \\ 1 & m = n \end{cases}$$

and R is the scalar appearing in (1.12).

We have shown how a measurement modifies the estimate and its statistics. It is thus apparent, that it is necessary to provide a starting estimate, and an associated covariance, to initiate the process. This has been done by using numbers which can be expected when performing the actual ALRS process. The apriori positions of the retroreflectors will have errors in each component which are dependent on the care taken in the process of target deployment.

The aircraft position may have an error standard deviation of 30 to 100 meters because of uncertainties in the LORAN/INS position location. Velocity estimates also have a random component.

The estimates of beam biases are zero; preliminary data show that the standard deviation about zero is less than 1 cm.

14

The estimates of atmospheric parameters have been made by assuming a monitoring station at a few retroreflector sites. A standard deviation of 1 mbar is used at the station, 100 mbar elsewhere. (i.e., tantamount to no knowledge of the meteorological information at the unmonitored site).

Extremely large prior covariances could be used, of course, implying heavier weighting of the ALRS data. One of the aspects of the data reduction which serves most to increase confidence in the ALRS approach is that estimation error variances are essentially independent of prior variances, provided that a one or more 1 mbar weather stations are used.

In the application of Kalman filtering to systems in which data is taken at discrete time points, processing is in two steps: incorporation of the new measurement data and propagation of the estimate between measurement points.

The discussion above has covered how the measurements are used. Between measurements all estimates (and true quantities) remain constant except for the aircraft. The aircraft position estimate is updated by applying the velocity over the time interval. For propagation of the co-variance, the studies reported here have taken the conservative stand that each new aircraft position has the same large error variance as does the initial position; thus assuming that the aircraft position determined by ALRS cannot be propagated. In actual data reduction, the estimated aircraft position may be used, thus improving accuracy; the difficulty of properly evaluating and modeling aircraft disturbances has led us to adopt a more conservative approach for analysis purposes.

3.3 Coordinates and Constraints

It is well known (12) that the multilateration problem, of which ALRS is an example, is not completely observable; that is, not all of the unknowns in the problem can be determined from the ALRS data. The simplest example of this is the fact that the same set of observations could be obtained if the complete set of aircraft and retroreflector positions were translated and

rotated as a rigid body. Thus there is a six-fold degeneracy in the problem. To avoid having some large variances in the covariance matrix while internal estimates become very accurate - a situation leading to numerical problems - an internal coordinate system has been defined for the estimation process. In this coordinate system, one retroreflector is chosen for the origin; one retroreflector defines the x-axis and therefore only its distance from the origin (its x-component) is estimated; and finally one retroreflector is taken to define the x-y plane. The variances are appropriately modified so that six components are perfectly known. It is important to note that the estimates, and variances of the estimates, of baseline length are independent of what coordinate system is chosen and, except for the numerical problem previously noted, no local coordinate system need be chosen.

These local estimates can be tied back to a larger coordinate system provided independently obtained coordinates in the larger system are available for at least three retroreflectors.

Baseline data (distance between retroreflectors) is intrinsically local data. When attempting to infer subsidence or expansion information it is necessary to define a plane with respect to which vertical motion can be measured. The ALRS local coordinate system defines this plane with the three "master" retroreflector locations.

4.0 RESULTS OF SIMULATION STUDIES

Simulations have shown that range measurements must be taken at two widely separated altitudes in order to strengthen the geometry sufficiently to recover baselines at the centimeter level. Thus, in a typical mission, the aircraft approaches the target grid at an altitude of 3.9 km as in Figure 4. After acquiring the first few targets, the instrument shifts to the tracking mode for the remainder of the mission. After overflying the rows of targets at 3.9 km, the aircraft climbs to its maximum cruise altitude (say 6 km) for a second set of passes over the target grid. The turning maneuvers between passes can be used to calibrate the on board attitude sensors.

AIRCRAFT
HIGH ALTITUDE

AIRCRAFT
LOW ALTITUDE

7 km

7 km

TARGET GRID
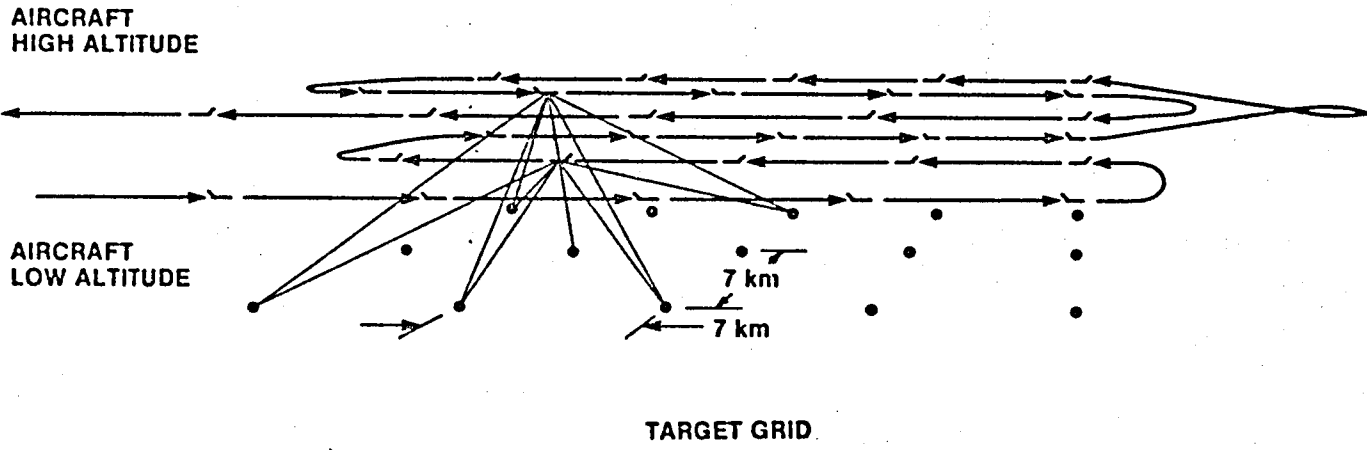
Figure 4. Typical ALRS Mission Scenario Perspective Showing Ranging from Two Different Altitudes

17

The spacing between targets will depend on several factors including the scientific objectives of the mission, the aircraft altitude, and terrain limitations. For the NP3A aircraft, the spacing is nominally taken to be 7 km. At typical cruise velocities (i.e., 200 knots), and at the most favorable aspect angle, laser range data to a given target is taken for approximately 300 seconds before the pointing system is commanded to acquire a new target. For a laser repetition rate of 10 pps, this corresponds to 3000 range measurements per target. Since a given target is common to a number of six target sets, and data are collected at two altitudes, over 6500 range measurements are typically made to each target.

Figure 5 illustrates the performance of the ALRS evaluated from error analyses. The baseline precision vs. baseline distance from an arbitrary origin is shown. The baseline precision decreases with increasing baseline length. For instance, in the absence of atmospheric refraction, the baseline precision is 0.65 cm for a 20 km baseline. The simulation was performed for a 15 target grid (3 by 5) under the assumption that the single shot laser range measurement uncertainty was ±1 cm RMS and the uncorrelated biases were on the order of ±1 cm. The total number of range measurements is 97,959 corresponding to the amount of data collected in approximately 27 minutes of flight time over the grid assuming no data dropout.

The baseline precision is degraded slightly in the presence of atmospheric refraction. The "with refraction" curve in the figure was determined under the assumption that surface pressure and temperature in the target region could be modelled by quadratic polynomials in the two surface coordinates and that the coefficients in the polynomials were determined by ground-based measurements of pressure and temperature at 15 locations (not coinciding with the target locations). It was further assumed that the surface measurements of pressure and temperature were accurate to ±1 mbar and ±1.4°C respectively. The vertical variation in pressure was assumed to be determined by the hydrostatic equation (13).
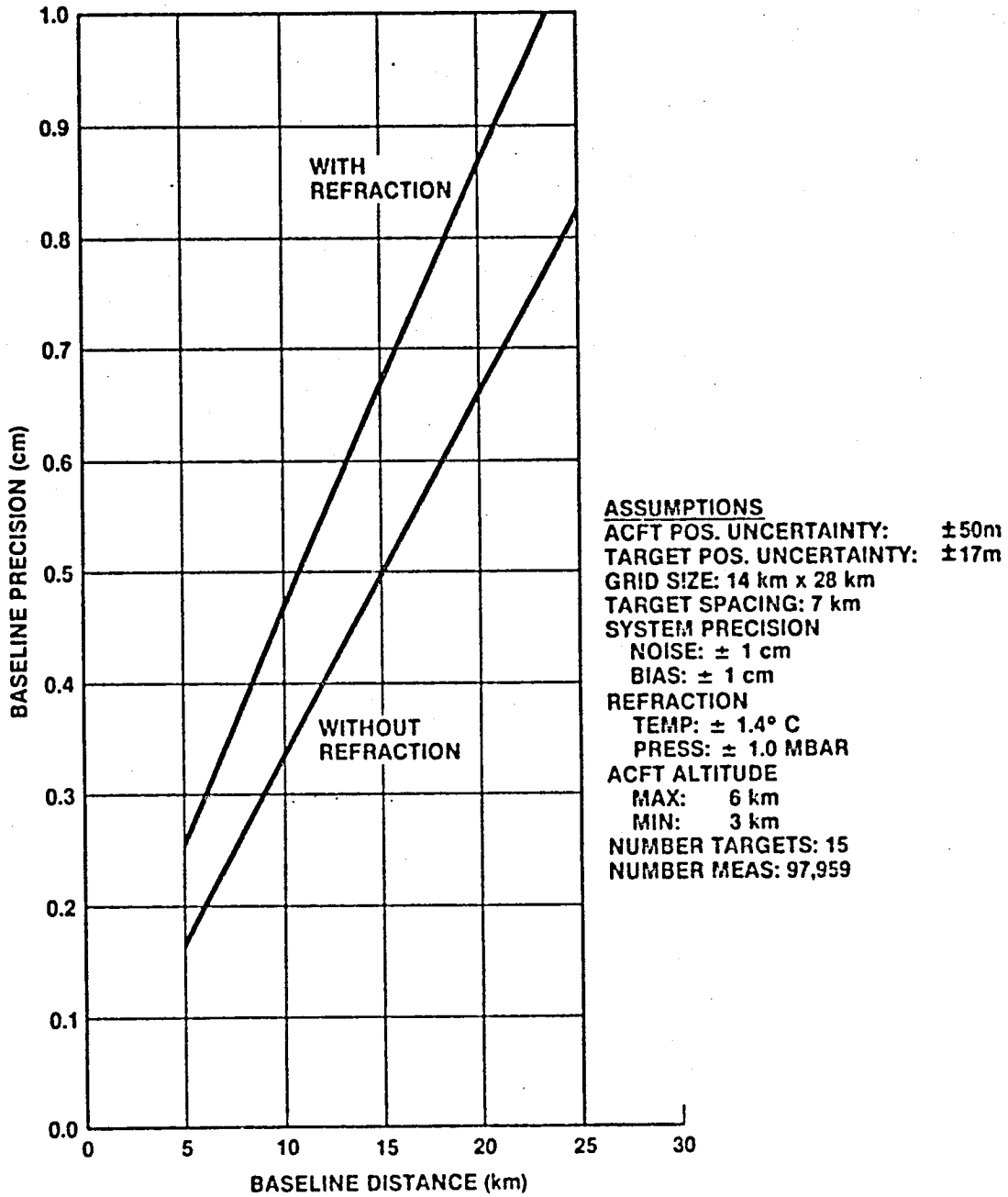
18

Figure 5. Baseline Precision vs. Baseline Distance

Figure 6 shows the importance of refraction errors and also illustrates that an extensive network of meteorological sensors is not required. Atmospheric measurements made at a single site co-located with a laser target within the ALRS grid, will significantly reduce the effects of atmospheric refraction upon ALRS baseline precision. In the estimation process described in Section 3, if the information from that single "met sensor" is used and the atmospheric parameters for the other ALRS targets are made part of the set of estimated parameters, a factor of about 7 improvement in baseline precision is achieved. The figure also shows that the inclusion of additional meteorological sensors within the ALRS target area does not significantly improve baseline precision. It should be emphasized that Figure 5 assumes an extensive meteorological sensing network in the neighborhood of the target region whereas Figure 6 utilizes meteorological sensors collocated at one or more target sites.

Figure 7 shows the evolution of baseline precision as a function of baseline distance for a region 14km X 112km in which 51 laser retroreflectors are deployed. It can be seen that the baseline precision is degraded at the rate of about 1.7 cm/100km. This result compares very closely with that obtained for smaller target grid areas.

In Figure 8 the evolution of baseline precision is given for a series of randomly deployed laser targets. These targets are distributed (as shown in the inset) in a potential ALRS flight test region in the vicinity of Shenandoah, VA. The targets were located at approximately 17 first order survey monuments currently maintained by the U.S. Geological Survey. The simulation indicates that the random target pattern does not significantly affect the baseline precision relative to that presented in Figs. 5, 6, and 7. For the simulation, one meteorological sensor was located in the middle of the grid and the meteorological parameters at other sites were determined in the estimation process.

AIRCRAFT ASSUMPTIONS
  MAXIMUM ALTITUDE: 6.0 km
  MINIMUM ALTITUDE: 3.9 km
  AVERAGE VELOCITY: 200 KNOTS

RANGING SYSTEM ASSUMPTIONS
  RMS NOISE: ± 1 cm
  BIAS UNCERTAINTY: ± 1 cm (SIX INDEPENDENT CHANNELS)
  SAMPLE RATE: 10 pps

ATMOSPHERIC MODEL ASSUMPTIONS
  STATION PRESSURES ARE UNCORRELATED
    (WORST CASE)
  PRESSURE UNCERTAINTY:
    ± 1 mbar AT MONITORED SITES
    ± 100 mbar AT UNMONITORED SITES

NUMBER OF
MEASUREMENTS: 97,959

NO METEOROLOGICAL STATIONS

ALRS GROUND
TARGET DISTRIBUTION

14 km

28 km

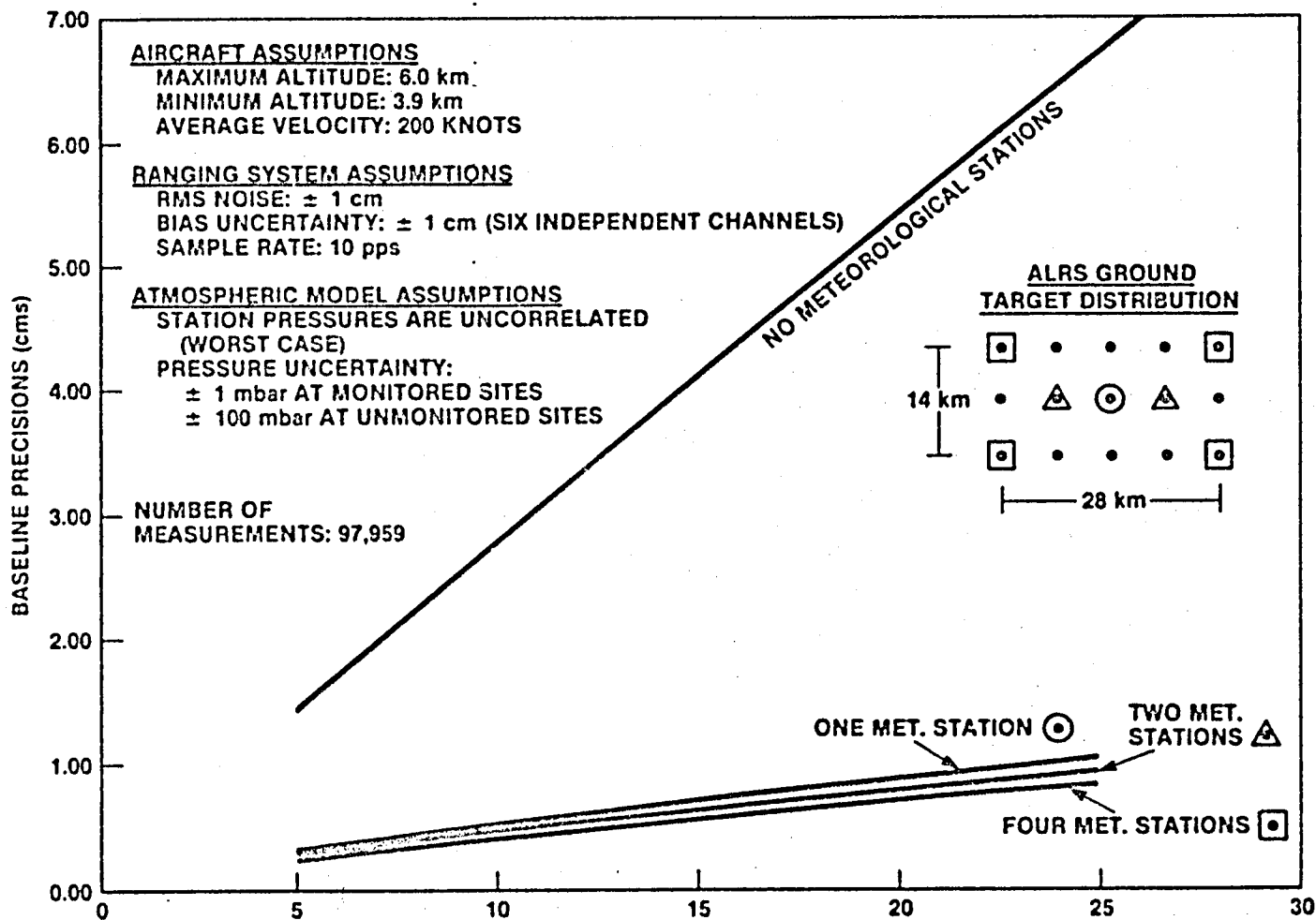ONE MET. STATION ⊙   TWO MET. STATIONS △

FOUR MET. STATIONS ▣

BASELINE PRECISIONS (cms)

Figure 6. Airborne Laser Ranging System Baseline Precision as a Function of the Number of Meteorological Stations
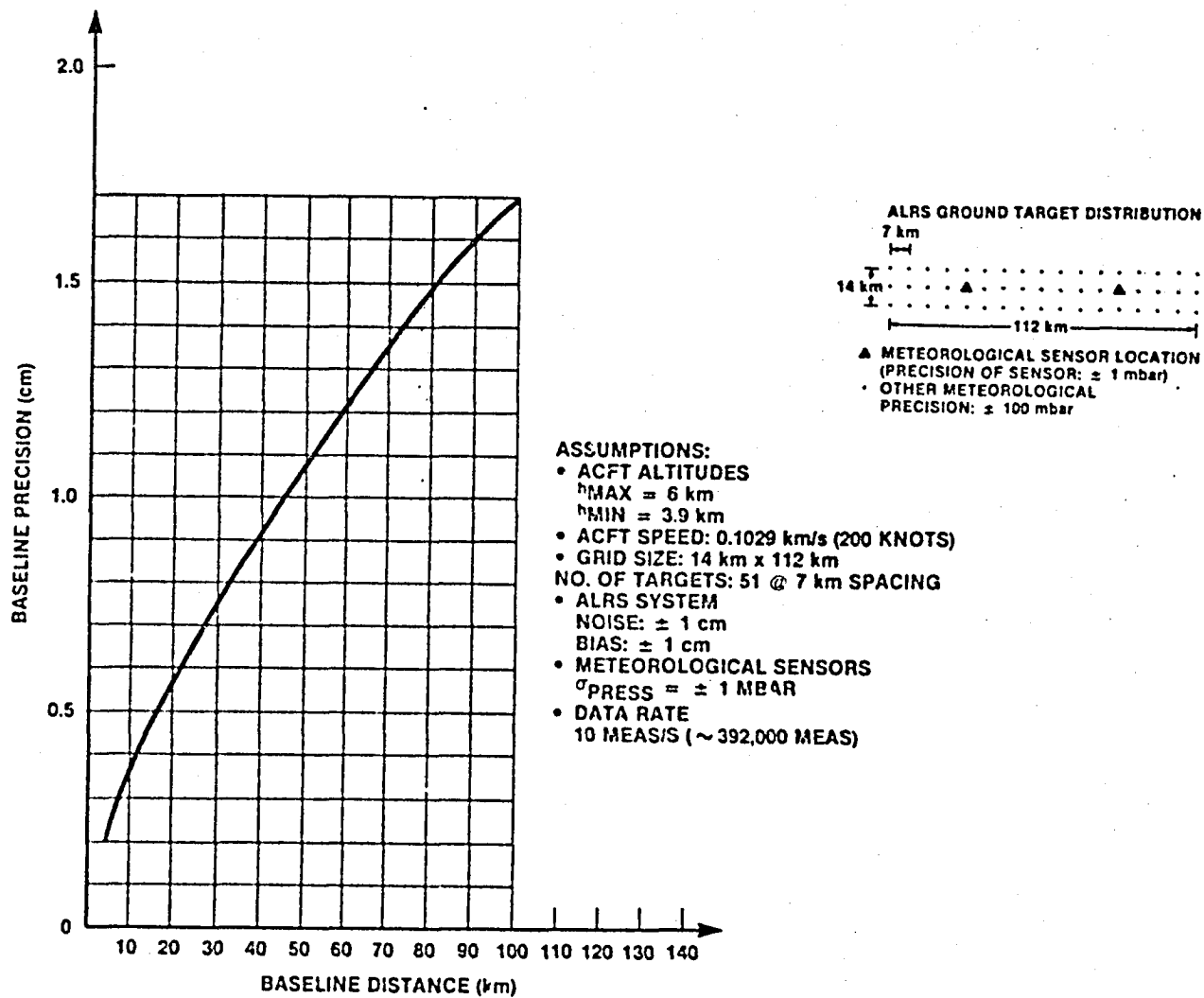
22

ALRS GROUND TARGET DISTRIBUTION

7 km

14 km

— 112 km —

▲ METEOROLOGICAL SENSOR LOCATION
(PRECISION OF SENSOR: ± 1 mbar)
· OTHER METEOROLOGICAL
PRECISION: ± 100 mbar

ASSUMPTIONS:
- ACFT ALTITUDES
  $h_{MAX} = 6$ km
  $h_{MIN} = 3.9$ km
- ACFT SPEED: 0.1029 km/s (200 KNOTS)
- GRID SIZE: 14 km x 112 km
NO. OF TARGETS: 51 @ 7 km SPACING
- ALRS SYSTEM
  NOISE: ± 1 cm
  BIAS: ± 1 cm
- METEOROLOGICAL SENSORS
  $\sigma_{PRESS} = \pm 1$ MBAR
- DATA RATE
  10 MEAS/S (~ 392,000 MEAS)

Y-axis: BASELINE PRECISION (cm) — 0, 0.5, 1.0, 1.5, 2.0

X-axis: BASELINE DISTANCE (km) — 10 20 30 40 50 60 70 80 90 100 110 120 130 140

Figure 7. Baseline Precision vs. Baseline Distance
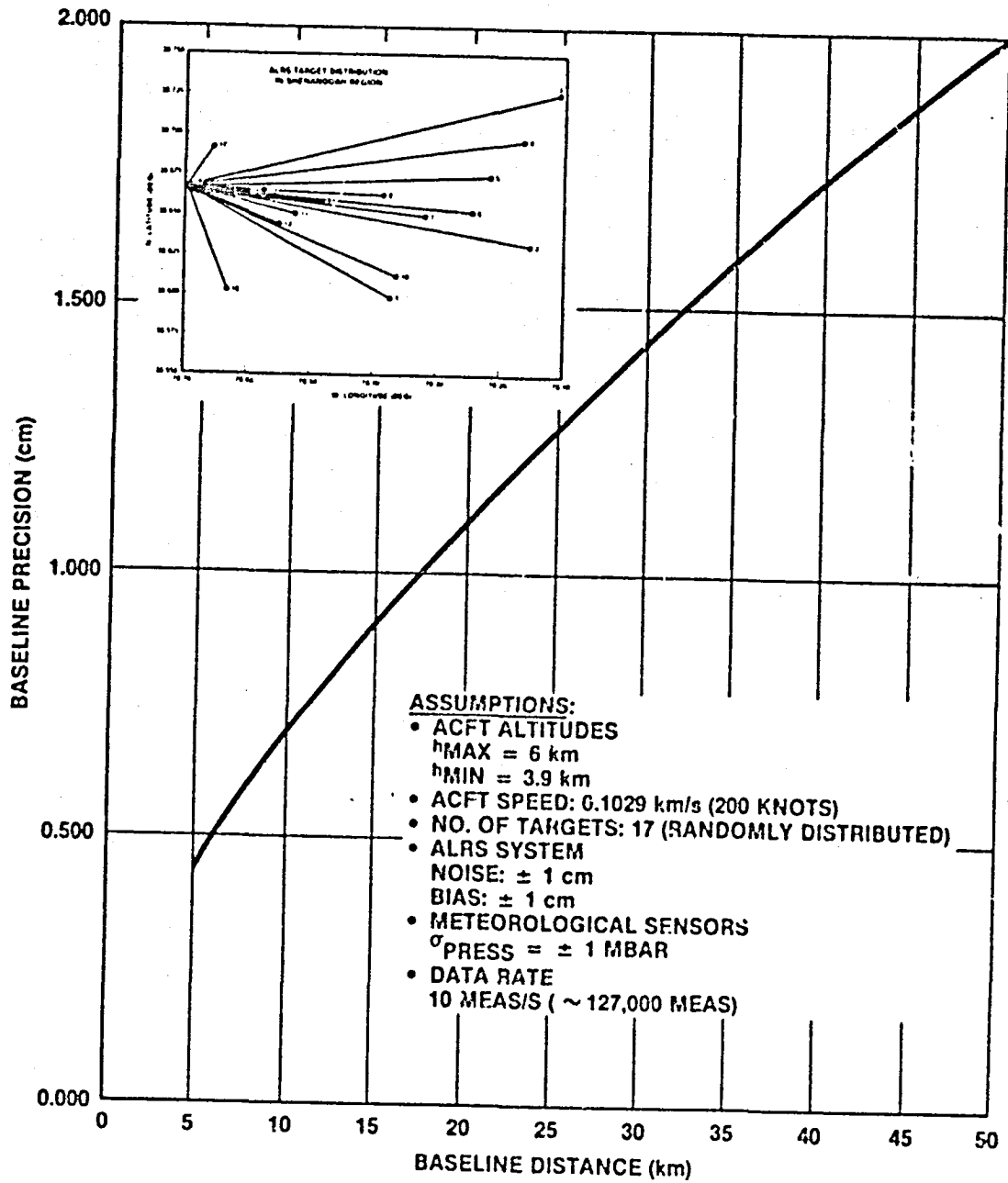
Figure 8. Airborne Laser Ranging System Baseline Precision for Random Laser Target Distribution

The figure's plotted axes and annotations read:

- Y-axis: BASELINE PRECISION (cm), marked 0.000, 0.500, 1.000, 1.500, 2.000
- X-axis: BASELINE DISTANCE (km), marked 0, 5, 10, 15, 20, 25, 30, 35, 40, 45, 50

ASSUMPTIONS:
- ACFT ALTITUDES
  h_{MAX} = 6 km
  h_{MIN} = 3.9 km
- ACFT SPEED: 0.1029 km/s (200 KNOTS)
- NO. OF TARGETS: 17 (RANDOMLY DISTRIBUTED)
- ALRS SYSTEM
  NOISE: ± 1 cm
  BIAS: ± 1 cm
- METEOROLOGICAL SENSORS
  σ_{PRESS} = ± 1 MBAR
- DATA RATE
  10 MEAS/S (~ 127,000 MEAS)

One of the principal applications anticipated for the ALRS surveying system is monitoring relative motion in the Earth's upper crust at the sub-centimeter/yr. rate. By developing and interpreting the system's ability to detect motions of the Earth's upper crust, a model of the strain accumulation compatible with observations of crustal motion and tectonics of a region within the experimental data collection area can be derived.

For example, for a target distribution as shown in Figure 7, baseline rate accuracies can be obtained from the baseline precision. By assuming that the baselines are measured over a one day period and by repeating the measurements every ninety days, then as shown in Figure 9, baseline rate accuracies at the end of a ten year observation period can be determined for 5 km baselines to better than 0.02 cm/yr and for 100 km baselines to about 0.1 cm/yr. These baseline rates correspond to strain rates of 4×10^{-8} strain/yr and 1×10^{-8} strain/yr. With the baseline rate accuracies indicated, the ALRS could provide a capability to observe the precursory geodetic motions believed to occur before large earthquakes. Indeed within a regional scale, the ALRS could provide the first real possibility of "capturing" a magnitude 7.5 and above earthquake.

CONCLUSIONS

The Airborne Laser Ranging System is a unique instrument capable of rapidly performing dense, large scale geodetic and engineering surveys with subcentimeter accuracies over long baselines. Since all data is initiated, received, and processed at the aircraft, there is no need for a complex data collection network, absolute time information, or skilled personnel in the field. It therefore promises to be a highly cost effective device for geophysics studies, large scale surveying, and land management applications, especially when combined with photogrammetric instrumentation. This system can detect strain rates to an accuracy of about 5×10^{-8} strain per year over a measuring period of 4 years. Such a system can therefore provide the capability to observe on a regional scale the precursory crustal motions believed to occur before large earthquakes.
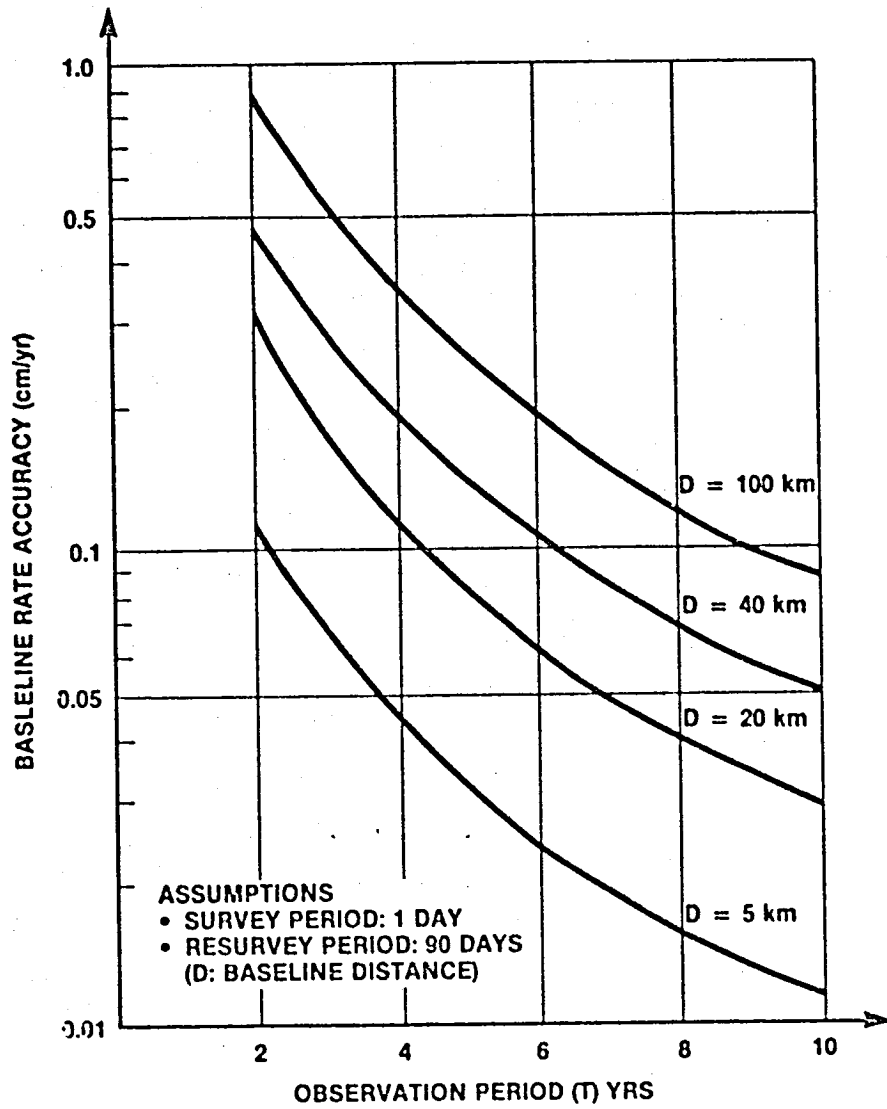
Figure 9. Baseline Rate Accuracy vs. Total Observation Period

ACKNOWLEDGMENTS

1. J. B. Abshire, "Pulsed Multiwavelength Laser Ranging System for Measuring Atmospheric Delay," Applied Optics, 19, pp. 3436–3440, October 1980.

2. M. W. Bird, R. D. Wierenga, and J. V. Tencate, "Kalman Filter Design and Performance for an Operational F-4 Loran Inertial Weapon Delivery System," presented at the 1976 National Aerospace Electronics Conference, Dayton, Ohio (May 1976).

3. A. E. Gaunt and D. L. Gray, "The AN/ARN-101 Loran Receiver," Proceedings of the Wild Goose Society (4 Townsend Rd., Acton, MA, 01720). 1975.

4. J. B. Abshire, J. L. Frisuey, and P. L. Fuhr, "Design and Operation of the Airborne Laser Ranging System (ALRS) Computer," NASA X-723-81-30, August 1981.

5. B. P. Gibbs and E. M. Haley, "Error Analysis of the Spaceborne Earth Applications Ranging (SPEAR) System," BTS-TA-77-48, September 1977.

6. C. S. Gardner, "Comparison Between the Refraction Error Covariance Model and Ray Tracing," University of Illinois, RRL Report 486, June 1977.

7. C. S. Gardner, "Statistics of the Residual Refraction Errors in Laser Ranging Data," University of Illinois, RRL Report 481, January 1977.

8. C. S. Gardner, "Corrections of Laser Tracking Data Effects of Horizontal Refractivity Gradients," Applied Optics, Vol. 16, September 1977, page 2427.

9. B. P. Gibbs and V. Majer, "Accuracy Assessment of Atmospheric Correction Used in the NASA Laser Ranging Program," BTS Report FR-81-166, September 1981.

10. B. P. Gibbs, "Evaluation of Polynomial Regression for Pressure and Temperature Data and Its Application to Laser Refraction Modelling," BTS TR-78-53, February 1978.

11. A. H. Jazwinski, "Stochastic Processes and Filtering Theory," Academic Press, 1970.

12. I. I. Mueller, B. H. W. Van Gelder and M. Kumar, "Error Analysis for the Proposed Closed Grid Geodynamics Satellite Measurement System (CLOGEOS)," Department of Geodetic Science Report No. 230, The Ohio State University, September 1975.

13. B. G. Gibbs and E. M. Haley, "Error Analysis of the Spacelab Geodynamics Laser Ranging System," Business and Technological Systems, Inc., BTS-TR-78-52, February 1978.

END

DATE

FILMED

MAY 5 1983

DO NOT REMOVE SLIP FROM MATERIAL

Delete your name from this slip when returning material to the library.

NAME	MS
Berkowitz	904

NASA Langley (Rev. May 1988)　　　　　　　RIAD N-75